Gas and Vapor Sorption, Permeation, and Diffusion in Glassy Amorphous Teflon AF1600

A. Yu. Alentiev,[†] V. P. Shantarovich,[‡] T. C. Merkel,[§] V. I. Bondar,[§] B. D. Freeman,[⊥] and Yu. P. Yampolskii*[,†]

A. V. Topchiev Institute of Petrochemical Synthesis, Russian Academy of Science, 29 Leninsky Pr., Moscow, Russia 119991; N. N. Semenov Institute of Chemical Physics, Russian Academy of Sciences, 4 Kosygina Str., Moscow, Russia 117977; Department of Chemical Engineering, North Carolina State University, Suite 3100, Partners II Building, 840 Main Campus Drive, Box 7265, Raleigh, North Carolina 27606; and Department of Chemical Engineering, Center for Energy and Environmental Resources, University of Texas at Austin, 10100 Burnet Road, Building 133, Austin, Texas 78758

Received March 28, 2002; Revised Manuscript Received July 30, 2002

ABSTRACT: Sorption and permeation parameters of light gases, C_1-C_{12} hydrocarbons, and C_1-C_7 perfluorocarbons were determined in a random, amorphous, glassy copolymer containing 65 mol % 2,2-bis(trifluoromethyl)-4,5-difluoro-1,3-dioxole (BDD) and 35 mol % tetrafluoroethylene (TFE) (TFE/BDD65 or AF1600). AF1600 results were compared to those of another copolymer, AF2400, which contains 87 mol % BDD. As the amount of bulky, packing-disrupting BDD increases, solubility coefficients increase systematically, primarily due to increases in the nonequilibrium excess volume of the glassy polymer. Permeability and diffusivity also increase with increasing BDD content. AF1600 is easily plasticized by larger, more soluble penetrants and is susceptible to penetrant-induced conditioning. As penetrant size increases, permeability and diffusion coefficients decrease. The rates of decrease of permeability and diffusivity with increasing penetrant size, which characterize permeability and diffusivity selectivity, are intermediate between those of conventional glassy polymers and exceptionally high free volume glassy materials such as poly(1-trimethylsilyl-1-propyne) (PTMSP). Positron annihilation lifetime spectroscopy (PALS) results suggest unusually large free volume elements and a bimodal distribution of free volume element size: this is consistent with similar results obtained earlier for other high free volume glassy polymers such as AF2400 and PTMSP. Inverse gas chromatography and PALS estimates of free volume element size distributions were consistent.

Introduction

Fluoropolymers have attracted attention as interesting gas separation membrane materials, primarily as a result of their extraordinary chemical stability and unusual permeation properties.[1−4] Several features of fluorine-containing polymers distinguish them from common hydrogen-containing polymers:

1. Perfluorinated substances (both low molecular mass liquids and polymers) are characterized by low cohesive energy density (CED) and, therefore, by enhanced gas solubility.[5] Additionally, as CED decreases, the activation energy of diffusion for small molecules, E_D, decreases (all other factors being equal),[6] so E_D values are relatively low in fluoropolymers.[4] On the other hand, the increase in E_D values and, in turn, decrease in diffusivity, with increasing penetrant size is less in polymers, such as fluoropolymers, with low CED than in polymers with higher CED.[6,7] Since permeability is often expressed as the product of solubility, S, and diffusivity, D:[8]

$$P = DS \tag{1}$$

these composite effects tend to increase permeability and decrease permeability selectivity.

2. Many highly fluorinated and particularly perfluorinated polymers are poorly soluble or even insoluble in all solvents except perfluorinated ones.[9] This property may present manufacturing difficulties for membrane formation because of the narrow range of solvents. However, once formed, such membranes have excellent chemical resistance and low tendency to swelling, which may yield better stability and longer membrane lifetime in chemically challenging environments.

Permeation properties of many fluorine-containing polymers have been studied. The most abundant information on structure/transport relations is available for polymers with aromatic backbones (e.g., polycarbonates (PC), polysulfones (PSF), and polyimides) containing $-C(CF_3)_2-$ (6F) groups in the main chain. Relative to analogous materials without 6F groups, these materials generally exhibit enhanced free volume and gas permeability combined with favorable values of permeability selectivity.[8,10] Similar effects may also be achieved by introducing fluoroalkyl groups as side chains in polymers.[11,12]

Much less information has been reported on the transport properties of perfluorinated polymers. Poly(tetrafluoroethylene) (PTFE) and copolymers of tetrafluoroethylene (TFE) and hexafluoropropylene (Teflon FEP) are semicrystalline, low permeability polymers that are considered barrier materials. For example, oxygen permeability coefficients for these polymers range from 1.3 to 1.6 barrers at ambient temperatures,[13] whereas for highly permeable polymers such as poly(1-trimethylsilyl-1-propyne) (PTMSP), oxygen permeability values may be larger by factors of 1000−

[†] A. V. Topchiev Institute of Petrochemical Synthesis, Russian Academy of Sciences.
[‡] N. N. Semenov Institute of Chemical Physics, Russian Academy of Sciences.
[§] North Carolina State University.
[⊥] University of Texas at Austin.
* Corresponding author: Tel 011.7.095.955.4210; Fax 011.7.095.230.2224; e-mail Yampol@ips.ac.ru.

10.1021/ma020494f CCC: $22.00
Published on Web 11/07/2002

10 000.[14,15] On the basis of these results, it was unexpected to observe very high gas permeability coefficients in random copolymers of tetrafluoroethylene and 2,2-bis(trifluoromethyl)-4,5-difluoro-1,3-dioxole, whose structure is the following:[1]

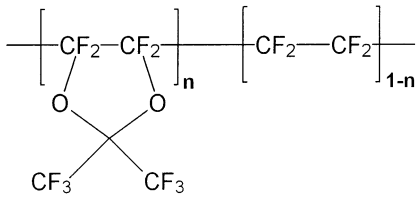

Teflon AF2400 and AF1600 are the names of copolymers where $n = 0.87$ and 0.65, respectively. Several recent studies have reported gas permeation and sorption properties as well as free volume of these amorphous glassy polymers.[2−4,16] AF2400 has been investigated in much more detail than AF1600.

The present paper extends the previous work on perfluorinated polymers and reports the results of a systematic study of sorption and gas permeation of a large series of gases and vapors including permanent gases, lower hydrocarbons, and fluorocarbons in amorphous AF1600. In addition, PALS was used to characterize free volume and the distribution of free volume in this polymer.

Experimental Section

Material. Teflon AF1600 was purchased from DuPont (Newark, DE) and used as received. It is a random copolymer containing 35 mol % TFE obtained via radical polymerization.[17] According to the supplier, its molecular mass is 100 000, the glass transition temperature is 156 °C, and the density is 1.7416 g/cm^3. Films having thickness from 15 to 150 μm were cast from solutions in perfluorinated hexanes (PF 5060, 3M Co., Minneapolis, MN) and from perfluorotoluene. Films for pure gas permeation and sorption measurements were dried at ambient conditions to constant weight. Chromatographic grade pure gases were used as received.

Permeation Measurement. Two types of permeation devices were used. A constant pressure/variable volume apparatus described previously[18] was employed at 35 °C with an upstream pressure in the range of 2−17 atm and a downstream pressure of 1 atm. Other details of the experimental procedure are reported elsewhere.[4] The second device used a Balzers QMG mass spectrometer for permeate gas detection.[19] Gas permeation was measured with an upstream pressure in the range of 0.1−1 atm and a downstream pressure near zero (10^{-3} Torr). In this instrument, time-lag determinations permitted the simultaneous determination of diffusivity and permeability coefficients.

Sorption Measurements. The sorption isotherms of gases and vapors were determined at 35 °C and pressures up to 27 atm with a barometric sorption apparatus.[20] Sorption isotherms were obtained for light gases (O_2, N_2, CO_2), lower hydrocarbons (CH_4, C_2H_6, C_3H_8, n-C_4H_{10}), and fluorocarbons (CF_4, C_2F_6). Before measurement, films were exposed to vacuum overnight to remove dissolved gases. The experiments were performed in a stepwise manner: after equilibrating the gas/polymer system at a fixed pressure, additional gas was introduced into the sample cell and equilibrium was reestablished. The sorption experiments were performed first on the light gases and then on vapor penetrants in the order of increasing critical temperature to avoid or minimized conditioning effects. Nitrogen sorption isotherms determined before and after each gas sorption isotherm agreed within experimental uncertainty, indicating no detectable conditioning effects.

In addition, the thermodynamics of vapor sorption in AF1600 was studied using inverse gas chromatography (IGC). Infinite dilution solubility and enthalpy changes of sorption for a series of n-alkanes (n-C_4H_{10} to $C_{12}H_{26}$) and perfluorinated solutes (C_6F_6 and $C_6F_5CF_3$) were determined using a gas chromatograph (LKhM-8MD) equipped with a flame ionization detector. The stainless steel column had a length of 1 m and an internal diameter of 1 mm. The polymer was coated over a solid carrier, SUPERINERTON, which was comprised of 0.125−0.16 mm diameter particles. The content of AF1600 on the surface of the solid carrier was 2 mass %. The carrier gas was helium, and methane served as a nonsorbing gas to characterize the dead volume of the chromatographic system. Inlet and outlet pressures of the column, measured by precision manometers, were used to correct retention volumes. No dependence of retention times or volumes on gas carrier velocity was noted, indicating that diffusion limitations were not significant. Therefore, all the retention parameters characterized sorption equilibrium in the system. For each solute, retention volumes were independent of sample size, indicating that infinite dilution conditions were realized. Liquid samples of chromatographic grade purity were used.

Positron Annihilation Lifetime Spectroscopy. The positron annihilation lifetime decay curves were measured at room temperature in an inert atmosphere using an Ortec "fast−fast" lifetime spectrometer. We used a nickel-foil-supported [^{22}Na] sodium chloride radioactive positron source. Two stacks of film samples, each with an overall thickness of about 1 mm, were placed on either side of the source. To perform measurements in an inert (nitrogen) atmosphere and to eliminate the contribution of additional orthopositronium decay due to the reaction with sorbed oxygen, which is important for high free volume materials, the sample and the source were placed in a plastic bag, which was then filled with dry nitrogen. The time resolution was 230 ps at full width half-maximum (fwhm). The contribution from annihilation in the source and instrumental resolution were taken into account in the CONTIN computing program, which gave a continuous lifetime distribution based on the experimental data. The integral statistics for each spectrum was equal to $(1.5−2.0) \times 10^7$ coincidences. In the CONTIN analysis, the probability density function of lifetimes $f(\tau)$ was obtained. It provides the probability that lifetimes are in the range of 50 ps in vicinity of a certain lifetime τ_i. The CONTIN spectral analysis program determined the chosen solution corresponding to regularization parameter value $\alpha \sim 10^{-4}$. This represents a solution having a Fisher F-probability closest to 0.5. The final PAL spectrum was obtained by summing the results of many cycles of measurements (10^6 counts in each cycle).

Results and Discussion

Gas Sorption. Sorption isotherms of gases and vapors at 35 °C are presented in Figure 1a−i. For comparison, the sorption isotherms in another copolymer, AF2400, having a higher content of bulky, packing disrupting BDD units, are also shown. All of the isotherms are concave to the pressure axis, which is consistent with the dual mode sorption (DMS) model:

$$C = C_D + C_H \tag{2}$$

$$C = k_D p + C'_H \frac{bp}{1 + bp} \tag{3}$$

where C is the total gas concentration in the polymer. C_D and C_H correspond to the Henry's law and Langmuir populations of sorbed molecules, respectively, in the polymer when the gas pressure is p. k_D is the Henry's law parameter characterizing sorption into the densified equilibrium matrix of the glassy polymer, C'_H is the Langmuir sorption capacity, which characterizes sorption into the nonequilibrium excess volume associated with the glassy state, and b is the Langmuir affinity

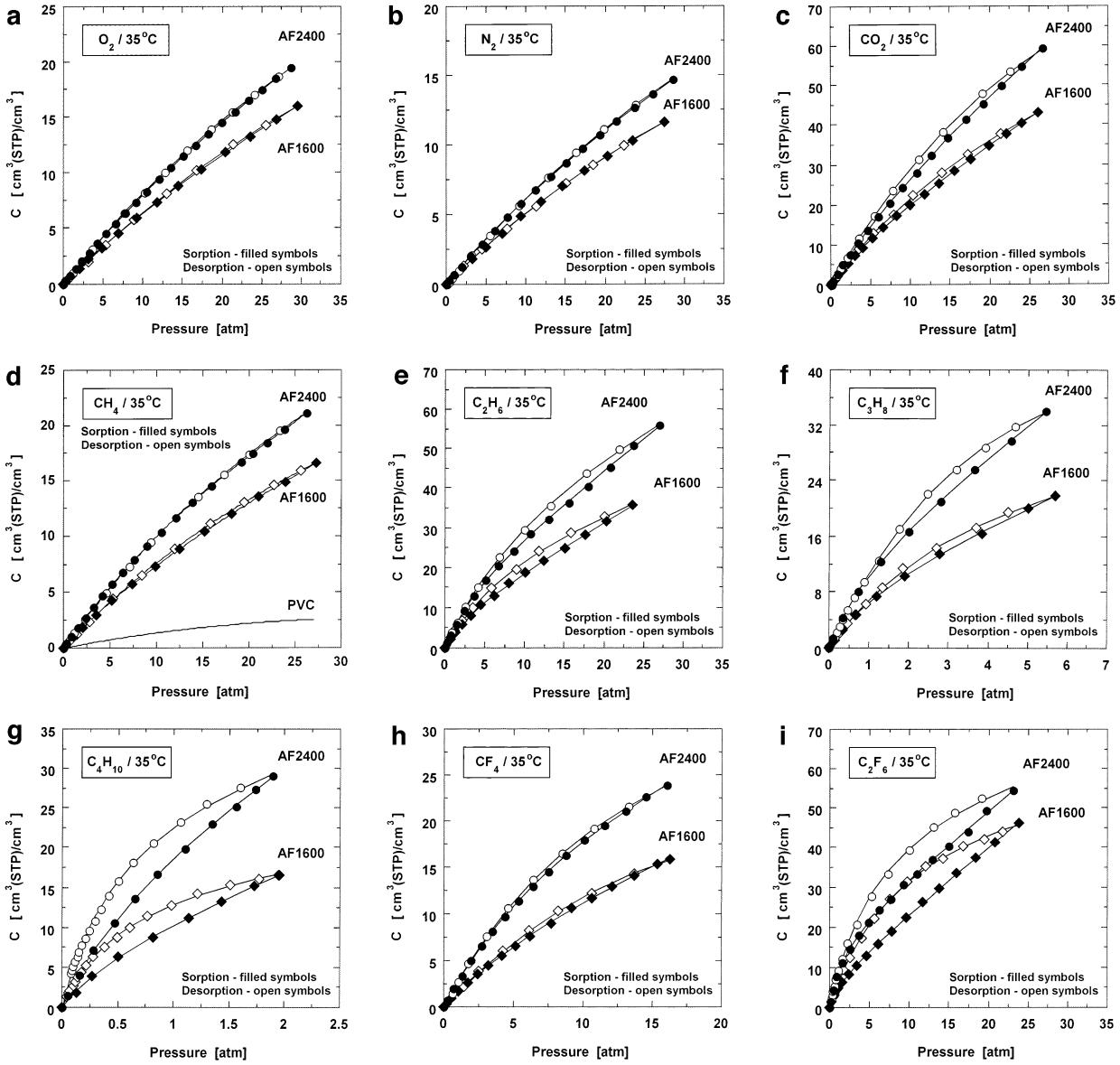

Figure 1. Sorption isotherms in AF1600, AF2400,[4] and (for CH_4) poly(vinyl chloride) (PVC) at 35 °C: (a) O_2, (b) N_2, (c) CO_2, (d) CH_4, line with no points−sorption isotherm in PVC,[21] (e) C_2H_6, (f) C_3H_8, (g) *n*-C_4H_{10}, (h) CF_4, (i) C_2F_6.

Table 1. Penetrant Molecular Properties and Dual-Mode Sorption Parameters of Several High Free Volume Glassy Polymers at 35 °C

parameter	polymer	O_2	N_2	CH_4	CF_4	CO_2	C_2H_6	C_2F_6	C_3H_8	C_3F_8
T_c [K]		154.6	126.2	191.0	227.5	304.2	305.3	297.5	370.0	345.1
V_c [cm^3/mol]		73.4	89.8	99.2	139.6	93.9	148.3	222.0	203.0	299.8
k_D [cm^3 (STP)/(cm^3 atm)]	PTMSP	0.19	0.08	0.50	0.78	1.05	1.3	0.96	5.3	2.0
	AF2400	0.44	0.15	0.35	0.45	1.6	1.5	1.6	4.2	6.4
	AF1600	0.30	0.20	0.42	0.53	1.22	1.16	1.65	2.23	
C'_H [cm^3 (STP)/cm^3]	PTMSP	80	74	62	27	130	71	34	60	29
	AF2400	13.3	37.6	24.5	29.3	25.5	16.2	17.8	13.2	19
	AF1600	16.5	14.8	8.1	12.2	15.4	9.7	7.7	11.9	
b [1/atm]	PTMSP	0.014	0.014	0.05	0.24	0.04	0.31	0.57	1.1	2.8
	AF2400	0.033	0.015	0.036	0.082	0.07	0.22	0.59	0.83	2.2
	AF1600	0.025	0.027	0.065	0.090	0.10	0.24	0.53	0.56	
S [cm^3 (STP)/(cm^3 atm)]	PTMSP	1.31	1.12	3.6	7.3	6.2	23.3	20.3	71.3	83.2
	AF2400	0.88	0.64	1.23	2.85	3.4	5.06	12.1	15.2	48.2
	AF1600	0.71	0.60	0.95	1.63	2.76	3.5	5.73	8.9	
$k_D/(k_D + C'_H b)$	PTMSP	0.14	0.07	0.14	0.11	0.17	0.06	0.05	0.07	0.02
	AF2400	0.50	0.23	0.28	0.37	0.47	0.30	0.13	0.28	0.13
	AF1600	0.42	0.33	0.44	0.33	0.44	0.33	0.29	0.25	

parameter. The model provides an excellent fit to the experimental sorption data, and the parameters resulting from a least-squares fit of the data to the model are recorded in Table 1. The lines in Figure 1 through the sorption data were drawn using the DMS parameters in Table 1.

All of the isotherms except those of lighter gases (e.g., O_2 and N_2) reveal hysteresis phenomena; i.e., desorption

isotherms are higher than sorption isotherms. The deviations are more pronounced for more soluble gases. For example, hysteresis is stronger for n-C_4H_{10} than for CH_4 or for C_2F_6 than for CF_4. Such behavior is observed in most studies of gas solubility in polymers below their glass transition temperature.[22] It is typically ascribed to rather long-lived increases in free volume resulting from sorption of high concentrations of solutes.[23] Solubility coefficients for all gases are larger in AF2400 than in AF1600. This result is consistent with the larger free volume of AF2400 as probed by PALS[3] and by density-based estimates of free volume.[4]

In Table 1, the DMS parameters are compared with DMS parameter values reported for AF2400[16] and PTMSP.[15] Comparison of these three polymers provides an indication of the effect of polymer chemical nature and free volume on sorption parameters. The higher sorption capacity of AF2400 than for AF1600 is due primarily to significantly larger values of C'_H in AF2400 for nearly all of the gases. This parameter characterizes the amount of nonequilibrium free volume in a glassy polymer,[8] and as mentioned, AF2400 has higher levels of free volume based on density and PALS results than AF1600.[3] Moreover, within a family of materials, C'_H values often increase with increasing glass transition temperatures,[24] and AF2400 has a higher T_g than AF1600. The two other parameters of the dual mode sorption model, k_D and b, differ in AF2400 and AF1600 rather insignificantly. The k_D and b values characterize the solute−gas equilibrium constants for the two populations of sorbed molecules: those dissolved in the more and less densely packed regions of the polymer, respectively. Therefore, the similar values of k_D and b in the two copolymers suggest similar polymer−solute interactions.

The Henry's law solubility coefficients of light gases (N_2, CO_2, CH_4) in the AF copolymers are several times larger than those of conventional glassy polymers (e.g., poly(vinyl chloride) (PVC), polystyrene (PS), PC, etc.).[24] The relatively large k_D values in AF2400 were ascribed to weaker intermolecular interactions in the perfluorinated matrix than in the hydrocarbon matrices of conventional polymers. This reasoning is analogous to that used to explain the high gas solubility in perfluorinated liquids.[5] The AF1600 results are also consistent with this explanation.

The Langmuir affinity parameter b characterizes the equilibrium adsorption in Langmuir sites. It often correlates[25] with solute critical temperature, T_c. However, studies of gas sorption in AF2400 and PTMSP showed[15] that the b values of the gases with very similar T_c values can differ by nearly an order of magnitude. Empirically, it was found that the sorbed molecule size, as characterized by critical volume V_c, was a better correlation parameter for b than T_c. A joint consideration of the results for three polymers and a series of gases (CO_2, C_2H_6, and C_2F_6) having similar T_c values but different V_c or van der Waals volumes V_w gives additional information on the role of this factor.

Table 2 presents the ratio of van der Waals volume[26] of these solutes to the sizes of free volume elements, V_f, measured by the PALS method in three polymers (PTMSP, AF2400, AF1600).[27] For the solute−polymer pairs examined, the following inequality holds: $V_f \gg V_w$. For a given polymer and a series of solutes with increasing size (e.g., CO_2, C_2H_6, C_2F_6) the ratio increases as V_w increases. It is evident that this ratio correlates with the Langmuir affinity parameters presented in Table 1. The same tendency is observed for another group of gases, C_3H_8 and C_3F_8. Therefore, when the size of solute molecules is getting comparable to the size of free volume element in polymers, the equilibrium is shifted to the "sorbed gas−site complex" as manifested in the increases in b values.

Table 2. Variation of the Ratio V_w/V_f for Different "Polymer−Solute" Pairs

	solutes with T_c = 297−305 K			solutes with T_c = 345−370 K	
polymer	CO_2	C_2H_6	C_2F_6	C_3H_8	C_3F_8
PTMSP	0.025	0.034	0.056	0.047	0.077
AF2400	0.037	0.051	0.085	0.071	0.115
AF1600	0.067	0.093	0.152	0.127	0.207

The ratio V_w/V_f does not correlate with the variations of the b parameter for the systems "one solute−different polymers". The Langmuir affinity parameter is an equilibrium constant, and it depends not only on the V_w/V_f ratio but also on the energetic state of the sites on the surface of the free volume element. It has to be assumed that the nature of polymers affects the b values more strongly than the nature of the sorbing gases.

According to eq 3, the solubility coefficient $S = C/p$ at infinite dilution, i.e., as $p \rightarrow 0$, is

$$S = k_D + C'_H b \tag{4}$$

As indicated in Table 1, solubility coefficients in AF1600 are systematically smaller than those of AF2400, in agreement with previous indirect measures of these values via permeability and diffusion coefficients.[3] Nevertheless, sorption levels in AF1600 are high relative to values observed in conventional glassy polymers. As a comparison, Figure 1d presents the sorption isotherm of methane in poly(vinyl chloride), a conventional low free volume glassy polymer.[21] Gas solubility coefficients larger than those of AF1600 and AF2400 are observed only for some high free volume substituted acetylene polymers.[15,28]

Previous studies of gas sorption in AF2400 showed that, at a given pressure, the concentrations of perfluorocarbons in this material are higher than those of analogous hydrocarbons.[4,16] A similar trend is observed for AF1600. For example, at 15 atm and 35 °C, the concentration of sorbed CF_4 is 15 and that of CH_4 is only 10 cm^3 (STP)/cm^3 polymer. The opposite behavior (i.e., hydrocarbon sorption being higher than fluorocarbon sorption) was observed in hydrogen-containing polymers such as PTMSP and poly(dimethylsiloxane).[7] This phenomenon has been ascribed to less favorable thermodynamics of dissolution of perfluorocarbons in hydrocarbon-based polymers and vice versa.

Inverse Gas Chromatography. Determination of solubility based on inverse gas chromatography (IGC) depends on measurement of retention times, t_r, of solutes in a column containing the polymer of interest. The t_r values are related to the net retention volume, V_N, as follows:

$$V_N = (t_r - t_a) J_n^{\,m} F_c \frac{273}{T} \tag{5}$$

where t_a is the retention time of a "nonsorbing" component (air or methane), $J_n^{\,m}$ is a correction factor for pressure drop in the column, F_c is the flow rate of gas

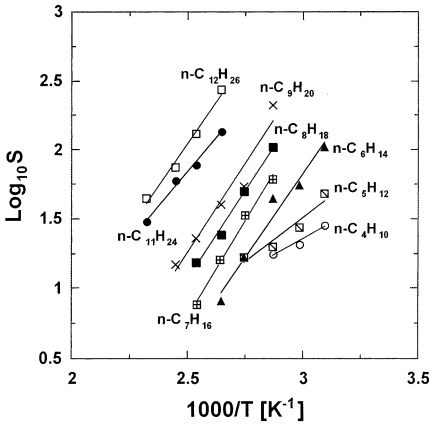

Figure 2. Temperature dependence of hydrocarbon solubility coefficients in AF1600.

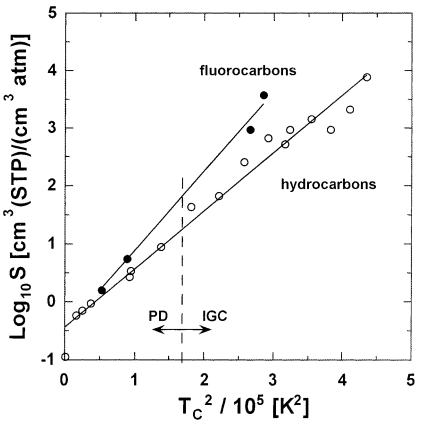

Figure 3. Correlation of infinite dilution solubility coefficients in AF1600 at 35 °C with critical temperature. Solubility coefficients were determined by pressure decay (PD) and inverse gas chromatography (ICG) methods.

carrier, and T is the column temperature (K). The specific retention volume, V_g, is defined as

$$V_g = \frac{V_N}{\omega_L} \tag{6}$$

where ω_L is the mass of the polymer in the column. Solubility coefficients in the infinite dilution limit, S, are given[29] by

$$S = V_g \frac{\rho}{p_0} \tag{7}$$

where p_0 is the standard pressure (1 atm) and ρ is the density of the polymer at temperature T. Taking into account nonideal gas behavior, eq 7 becomes

$$S = V_g \frac{\rho}{p_0} \exp\left[(2B_{11} - V_1)J_n{}^m \frac{p_0}{RT}\right] \tag{8}$$

where B_{11} is the second virial coefficient and V_1 is the solute molar volume. From the temperature dependence of S, the enthalpy of sorption can be estimated as follows:

$$S = S_0 \exp\left[-\frac{\Delta H'_s}{RT}\right] \tag{9}$$

Vapor dissolution in a polymer may be viewed as a sequence of two steps: penetrant condensation to a pure liquid state and mixing of the pure liquid with polymer. Hence, the enthalpy of sorption can be represented as

$$\Delta H_s = \Delta H_c + \Delta H_m \tag{10}$$

where ΔH_c and ΔH_m are enthalpies of condensation and mixing, respectively.

Figure 2 presents temperature dependences of the solubility coefficients found via eq 8 of several solutes in AF1600. These data obey eq 9 over the temperature range of study. Table 3 presents a comparison of retention volumes in AF1600 and AF2400 at 150 °C. On the basis of these data, AF1600 exhibits markedly lower solubility coefficients (i.e., lower retention volumes) than AF2400, which is consistent with the results of gas sorption studies using the pressure decay method.

In this study, we use pressure decay sorption and IGC to determine the solubility for a wide variety of solutes, ranging from nitrogen to *n*-dodecane. Solute physical parameters vary significantly: critical temperatures

Table 3. Specific Retention Volumes of Hydrocarbon Solutes at 150 °C in AF1600 and AF2400

	specific retention volume (cm^3/g)	
solute	AF2400	AF1600
n-hexane	10.0	1.2
n-heptane	18.7	1.6
n-octane	23.3	3.1
n-nonane	46.8	4.8
n-decane	84.3	14.0
benzene	17.3	1.8

range from 126 to 659 K and critical volumes range from 73 to 718 cm^3/mol. The experimentally determined solubility coefficients cover 4 orders of magnitude. These data, from two complementary experimental methods, enable one to assess the consistency of the results of the two methods and present an opportunity to reexamine the relationship between S and T_c. Figure 3 presents infinite dilution solubility coefficients in AF1600 at 35 °C as a function of critical temperature squared. Excellent consistency is observed between results of the pressure decay and IGC methods. Within each family of solutes (i.e., hydrocarbons and fluorocarbons), there is a strong linear correlation between the logarithm of solubility and critical temperature squared. This result suggests that the classic approach of correlating infinite dilution solubility with T_c (rather than $T_c{}^2$) is valid only approximately for solute sets having a narrower range of T_c values than those presented in this study. A similar result has been obtained for AF2400 and for semicrystalline polyethylene.[30] A least-squares treatment of the data for the hydrocarbon penetrants in Figure 3 yields the following result:

$$\log S\ (\mathrm{cm^3\,(STP)/(cm^3\ atm)}) = 1.00 \times 10^{-5} T_c{}^2\ (\mathrm{K^2}) - 0.43 \tag{11}$$

Solubility coefficients measured at different temperatures obey the following correlation with reduced critical temperature squared as suggested by Stern et al.[30]

$$\log S\ (\mathrm{cm^3\,(STP)/(cm^3\ atm)}) = M + N(T_c/T)^2 \tag{12}$$

In Table 4, parameters for eq 12 are presented for several polymers. It is worthwhile to note that independent of the chemical nature and physical state of polymers (amorphous glassy or rubbery, semicrystalline) similar slopes are observed. On the other hand, the intercept M exhibits more variation from polymer to

Table 4. Parameters for Solubility Corresponding States Relation (Eq 13) for Several Polymers

polymer	type of material	*N*	*M*
AF1600 (this work)	amorphous glass	0.95	−0.43
AF2400[4]	amorphous glass	1.11	−0.35
polyethylene[30]	semicrystalline, rubbery amorphous phase	1.14	−1.29
poly(dimethylsiloxane)[31]	amorphous rubber	1.075	−0.75
poly(dimethylsilmethylene)[32]	amorphous rubber	1.123	−0.939
poly(dimethylsiltrimethylene)[32]	semicrystalline, rubbery amorphous phase	1.175	−0.829

Table 5. Sorption Enthalpies of *n*-Alkanes in AF1600

solute	ΔH_s (kJ/mol)	ΔH_m (kJ/mol)	solute	ΔH_s (kJ/mol)	ΔH_m (kJ/mol)
n-C_4H_{10}	−18.1 ± 0.6	4.3	*n*-C_9H_{20}	−49.1 ± 0.7	−11.3
n-C_5H_{12}	−24.6 ± 0.5	1.2	*n*-$C_{10}H_{22}$	−34.7 ± 0.5	−4.6
n-C_6H_{14}	−46.3 ± 0.6	−17.5	*n*-$C_{11}H_{24}$	−47.3 ± 0.7	−5.8
n-C_7H_{16}	−52.0 ± 0.6	−20.3	*n*-$C_{12}H_{26}$	−40.7 ± 0.5	2.9
n-C_8H_{18}	−48.7 ± 0.5	−14.3			

polymer. Larger *M* values are observed for AF1600 and AF2400, the only glassy materials included in the comparison. This result is consistent with the well-known tendency for higher gas and vapor solubility in glassy polymers than in rubbery polymers.

Figure 3 shows that solubility of fluorocarbons in the perfluorinated material AF1600 is systematically higher than those of hydrocarbons. This conclusion is based on the results of both pressure decay and IGC experiments. It is well-known that liquid hydrocarbon solvents show smaller solubility of fluorocarbons as compared to that of hydrocarbons. For example, the solubility of C_2F_6 in cyclohexane is lower by 1 order than the solubility of ethane.[5] Recently, the same effect was demonstrated for the solubility of fluorocarbon and hydrocarbon gases in hydrocarbon-based polymers—rubbery poly(dimethylsiloxane)[33] and glassy PTMSP.[15] A conclusion on less favorable of mixing of fluorocarbon gases in hydrocarbon media was made.[33] An opposite behavior indicative of favorable thermodynamic interactions was observed for two perfluorinated polymers studied—amorphous Teflons AF2400 and AF1600 (ref 16 and this work).

As both amorphous Teflons are glassy polymers, an interpretation based on the dual-mode sorption parameters can be also given. Enhanced solubility coefficients in glassy polymers described by formula 4 can be attributed to the second (Langmuir) term $C'_H b$. An examination of Table 1 indicates that fluorocarbon components of the pairs with similar critical temperatures (e.g., CF_4 and CH_4) are characterized by larger values of the C'_H and *b* parameters. This regularity is observed in both perfluorinated polymers.

Enthalpies of sorption of aliphatic hydrocarbons in AF1600 are presented in Table 5. The ΔH_s values are strongly negative, with the smallest alkanes having the least negative values. This result is due to the systematically more exothermic ΔH_c values with increasing carbon number[34] coupled with ΔH_m values that exhibit a minimum, near *n*-C_7H_{16} for AF1600, as a function of carbon number. Such behavior has also been observed for AF2400[16] and other glassy polymers.[35] We will return to this point in the next section.

Positron Annihilation Estimate of Free Volume Size Distribution. PALS is a unique method for direct probing of free volume in polymers.[36] When positrons enter a polymer medium, they exist until annihilation as free positrons, e^+, or as hydrogen-like positronium particles, e^+-e^-. Orthopositronium (o-Ps) particles have parallel spins of e^+ and e^- and a lifetime of 142 ns in a vacuum. However, in condensed matter such as polymers, o-Ps annihilates much faster (ca. 1−10 ns) due to interactions with surrounding electrons. Numerous PALS studies of glassy and rubbery polymers showed that positron lifetime distribution includes a single o-Ps or long-lived component, τ_3, whose lifetime is in the range 1.5−3.5 ns. On the other hand, in some highly permeable, high free volume polymers, a second, much longer lifetime, τ_4 was observed, and it could be as large as 14 ns.[27,37,38] Consistent with this observation, bimodal o-Ps lifetime distributions are observed in such materials if the PALS data are fit to a continuous lifetime distribution model. Bimodal lifetime distributions could also be observed in glassy polymers with more common permeability, diffusivity, and free volume properties.[27]

A semiempirical model was proposed[36] for estimating the average radii of free volume elements from o-Ps lifetimes:

$$\tau_i = {}^1/_2[1 - (R_i/R_0) + ({}^1/_2\pi)\sin(2\pi R_i/R_0)]^{-1} \quad (13)$$

where $\tau_i = \tau_3$ or τ_4 are o-Ps lifetimes (ns) and $R_i = R_3$ or R_4 (Å) are the radii of free volume elements. $R_0 = R_i + \Delta R$, where $\Delta R = 1.66$ Å is an estimate of the electron layer thickness. This model is based on equivalent spherical free volume elements.

The size distribution of free volume elements in AF1600 obtained using the CONTIN program, which is the probability density function $f'(R)$, is presented in Figure 4. A bimodal distribution is observed. The smaller free volume elements (R_3 ca. 3 Å) have a size similar to those in conventional glassy polymers. The larger free volume elements, whose radii, R_4, are centered near 5−6 Å, are similar to those reported in such polymers as PTMSP and AF2400.[3,38] Within the context of the model in eq 13 (i.e., equivalent spherical free volume elements), the average volume of a free volume element would be in the range 500−900 Å^3.

It will be quite important to compare PALS results with other experimental estimates of free volume element size in polymers. However, it is very rare to find such comparisons in the literature. In the present case, however, we may compare results from IGC with the

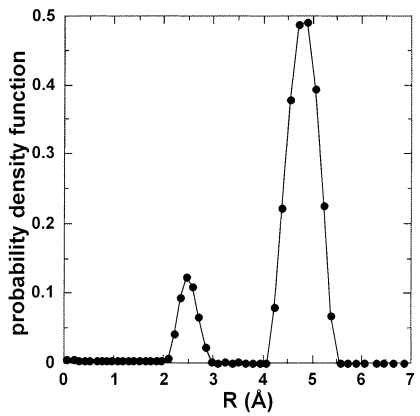

Figure 4. Size distribution of free volume elements in AF1600 as probed by positron annihilation lifetime spectroscopy.

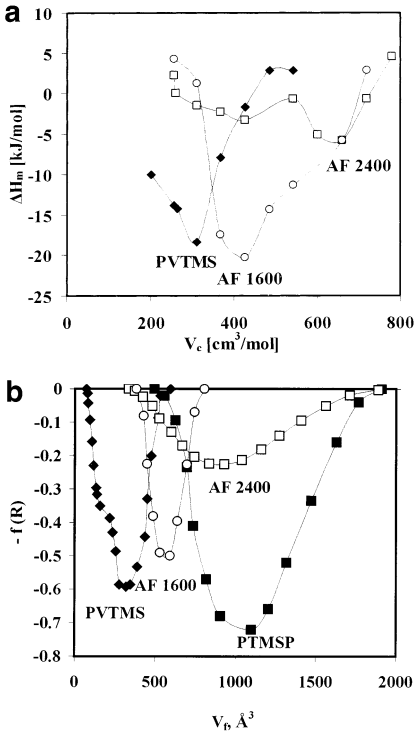

Figure 5. Estimation of the size of free volume elements in glassy polymers: (a) excess enthalpy of mixing ΔH_m as a function of critical volume of solute V_c according to IGC; (b) probability density function $f(R)$ in polymers with different size of free volume elements according to PALS.

PALS results. Prior IGC studies of several glassy polymers showed that the excess functions of mixing (e.g., ΔH_m) are strong nonlinear functions of solute (probe) size.[35] ΔH_m decreases with increasing solute size (as characterized by, for example, van der Waals volume, V_w, or critical volume V_c) up to a limiting value of solute size. Then, ΔH_m values pass through a minimum and increase strongly with increasing solute size. Such behavior has been reported for poly(vinyltrimethylsilane) (PVTMS),[35] AF2400,[16] and, in this work, for AF1600. Near the minimum, the mixing is strongly exothermic. In contrast, the mixing becomes only weakly exothermic or thermoneutral for larger solutes. It was hypothesized that such behavior resulted from the ability of free volume elements to accommodate most efficiently solute molecules smaller than the intrinsic size of free volume elements. Minimum intermolecular forces would be overcome to accommodate such solutes, so negative ΔH_m values would be observed. The more similar the size of a sorbed molecule is to that of the free volume elements, the more restrictions are imposed on the internal degrees of freedom of the sorbed molecule within the free volume elements. Thus, it was assumed that the coordinates of the ΔH_m minimum vs solute volume provide estimates of the size of free volume elements. Now it is possible to check these assumptions using the comparison with PALS results.

Figure 5a shows the effect of critical volume on the excess enthalpy of mixing, ΔH_m, in three polymers: AF1600, AF2400, and PVTMS. The curves for the two latter polymers are given according to ref 16. Critical volume was selected as a convenient parameter to characterize solute size. *n*-Alkanes were used as probes in Figure 5a. It can be noted that ΔH_m passes through a minimum for each polymer, and the positions of the minima, $V_{c,min}$, are qualitatively consistent with gas permeability and diffusivity of the polymers considered. That is, the polymer with the highest $V_{c,min}$ has the highest diffusivity and permeability and vice versa.

Table 6. Radii of Spherical Free Volume Elements (Å)

	method	
polymer	IGC	PALS
PVTMS	5.3	4.4
AF1600	5.5	5.2
AF2400	6.4	6.0
PTMSP		6.4

Figure 5b presents schematically the size distribution of larger free volume elements obtained from CONTIN lifetime distributions. For more convenient comparison, the ordinate of Figure 5b shows the values $-f(R)$, where $f(R)$ is the probability density function found using CONTIN lifetime distribution and eq 13. Based on free volume radius distribution like the one shown in Figure 4, corresponding volume distributions were calculated for the approximation of spherical geometry of free volume elements V_f (Å^3).

A comparison of parts a and b of Figure 5 shows a thorough analogy between the results of both methods.

1. The relative positions of the curves in both plots are very similar. According to the two methods, the minimum size of free volume elements is characteristic for PVTMS and maximum for AF2400. For AF1600 and PVTMS, the curves $\Delta H_m(V_c)$ pass through maxima for C_6-C_7 alkanes, whereas the maximum for AF2400 occurs at much larger solutes (ca. $C_{10}-C_{11}$).

2. Based on the PALS results in Figure 5b, AF1600 exhibits a much narrower size distribution of free volume element sizes than AF2400. Presumably, the narrower the distribution, the more drastic will be the segregation of sorbed molecules based on size. In fact, this notion is supported by the IGC-based estimates of ΔH_m: as shown in Figure 5a, the minimum in ΔH_m is much wider in AF2400 than in AF1600.

In Table 6, the comparison is made of the radii of supposedly spherical free volume elements in AF1600 and other polymers as estimated using the IGC and PALS methods. Bearing in mind approximate assumptions about the geometry of free volume elements in polymers (see e.g. ref 39), the agreement between R(IGC) and R(PALS) should be considered as quite reasonable.

Gas Permeability. The permeability of AF1600 to the following series of gases was determined at 35 °C and upstream pressures ranging from 2 to 17 atm: H_2, O_2, N_2, CO_2, CH_4, C_2H_6, CF_4, and C_2F_6. Films for these experiments were cast from solution in PF 5060. In addition, permeability coefficients were also measured for He, H_2, O_2, N_2, CO, CO_2, CH_4, and SO_2 in the temperature range from 19 to 50 °C at subatmospheric pressure. Films for these experiments were cast from solution in perfluorotoluene.

As shown in Figure 6, the permeability coefficients of light gases are independent of pressure, which is typical for supercritical gas permeability in polymers.[8] Permeability coefficients begin to depend more significantly on pressure for C_2 and larger (i.e., more condensable) penetrants. Interestingly, the pressure dependence is markedly stronger for C_2F_6 than for C_2H_6: the permeability coefficient of C_2H_6 increases about 2-fold over the pressure range studied whereas C_2F_6 permeability increases by a factor of ca. 8. Presumably, this behavior is related to the larger solubility of the per-

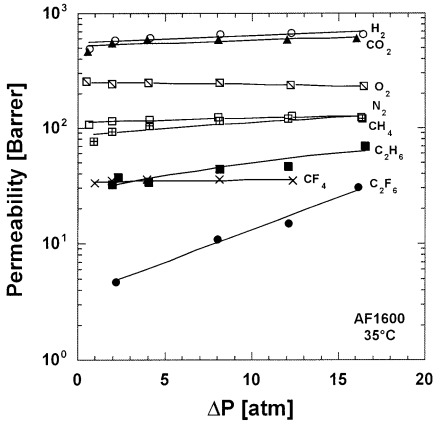

Figure 6. Effects of pressure on gas permeability in AF1600 at 35 °C. Δp is the difference between upstream pressure and downstream pressure, which is maintained at 1 atm in these experiments.

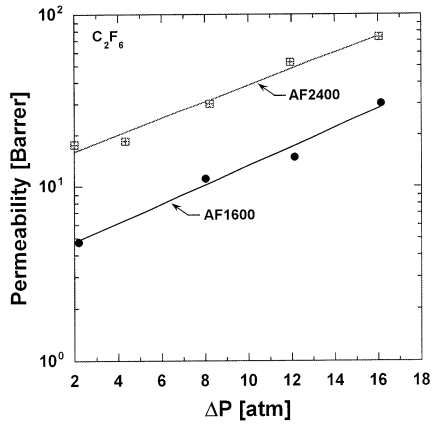

Figure 7. Effect of pressure on perfluoroethane permeability coefficients in AF1600 and AF2400 at 35 °C.

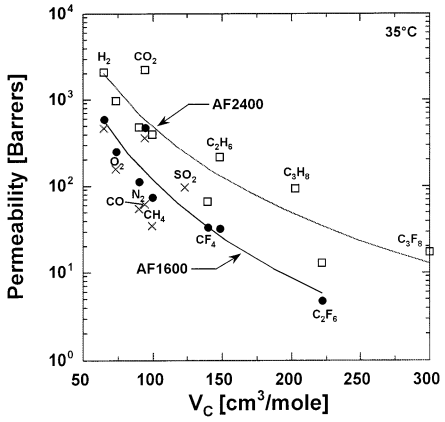

Figure 8. Infinite dilution permeability coefficients as a function of critical volume V_c at 35 °C in AF2400[4] (□) and AF1600. The AF1600 data were determined using both high-pressure techniques (●) and the subatmospheric method (×).

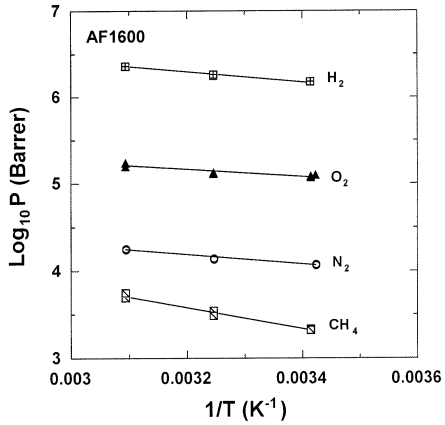

Figure 9. Arrhenius dependence for permeability coefficients in AF1600.

fluorocarbon in AF1600 (cf. Figure 1) and more pronounced plasticization of the polymer by the fluorocarbon solute. A similar pressure dependence of permeability coefficients has been reported for AF2400.[4] Figure 7 illustrates the effect of pressure on the permeability of C_2F_6 in these two polymers. The two lines have approximately the same slope, and the lower permeability of AF1600 is due to smaller solubility and diffusion coefficients, as will be discussed shortly.

Figure 8 presents permeability coefficients of AF1600 as a function of penetrant size at $\Delta p = 0$. For comparison, AF2400 data[4] are also shown. There is a reasonable agreement between the data points measured using the different experimental techniques (i.e., subatmospheric mass spectrometer detection and high-pressure direct flux measurement). The low-pressure measurements generally yield somewhat lower gas permeability, which may be due to sensitivity of permeability coefficients to differences in film casting protocol. Such effects have been reported for AF2400.[4]

Often, penetrant size exerts a strong influence on permeability coefficients in rubbery and glassy polymers.[40,41] In general, the permeability coefficients of light gases (e.g., He, O_2, and N_2) decrease with increasing penetrant size. For larger penetrants, e.g. C_1-C_4 hydrocarbons, permeability coefficients increase with increasing penetrant size in many rubbery or weakly size-sieving glassy polymers (i.e., PTMSP) and decrease with increasing penetrant size in strongly size-sieving materials, like conventional glassy polymers (e.g., polysulfone or polycarbonate). From Figure 8, the behavior of AF1600 and AF2400 is similar to that in conventional glassy polymers despite the rather high gas permeability. For all the penetrants, the permeability of AF1600 is markedly lower than that of AF2400. The permeability coefficients of CO_2 measured by both methods in AF1600 and AF2400 deviate significantly from the smoothed line drawn through the data points. Similarly, the permeability coefficients of SO_2 are also larger than the general trend for other gases. This phenomenon is due, in part, to the much higher solubility coefficients of these penetrants relative to the solubility of other penetrants of similar size. For example, the solubility coefficient of CO_2 in AF1600 and AF2400 is much larger than that of N_2, which has a rather similar critical volume. As discussed earlier, solubility depends on penetrant size and condensability, which is characterized by critical temperature. Carbon dioxide and sulfur dioxide have much larger T_c values than penetrants having approximately the same size (i.e., N_2 and CH_4).

The effects of temperature on permeability coefficients of several gases in AF1600 are presented in Figure 9. The activation energies of permeation determined from these data are recorded in Table 7. For certain very large free volume materials, such as PTMSP, permeability coefficients of even light gases decrease with increasing temperature (i.e., activation energies of permeation are negative).[42−44] For the gases studied except CO_2, the activation energies in AF1600 are

Table 7. Activation Energies of Sorption and Transport in AF1600

gas	E_P (kJ/mol)	E_D (kJ/mol)	ΔH_s (kJ/mol)
He	4.4		
H_2	4.8		
O_2	3.4	8.4	−5.0
N_2	4.6	12.0	−7.4
CO	5.9	15.5	−9.6
CO_2	−1.8	15.0	−16.8
CH_4	10.3	18.4	−8.1
SO_2	2.7	18.1	−15.4

positive, though somewhat lower than values for conventional glassy polymers such as polyimides.[45] Because[8]

$$E_P = E_D + \Delta H_s \tag{14}$$

low values of E_P can be due to low E_D and/or highly exothermic enthalpy of sorption ΔH_s. Low activation energies of diffusion are characteristic of high free volume polymers. In AF1600, E_D values are significantly smaller that those of conventional low free volume, glassy polymers. For example, $E_D(O_2)$ and $E_D(N_2)$ in PC are about 32 and 40 kJ/mol, respectively,[13] while in AF1600, the activation energies for diffusion of O_2 and N_2 are only 8.4 and 12 kJ/mol. Since the ΔH_s values in AF1600 are also more negative than in conventional glassy polymers, these two factors combine to yield small or even negative E_P values.

Diffusivity. Two methods were employed to determine diffusion coefficients. Concentration-averaged diffusion coefficients, D_a, were estimated from the high-pressure permeability and sorption data as follows:

$$D_a = P(p_2 - p_1)/(C_2 - C_1) \tag{15}$$

where P is the pressure-dependent permeability coefficient measured at upstream and downstream pressures of p_1 and p_2, respectively, and C_1 and C_2 are the equilibrium penetrant concentrations sorbed by AF1600 at p_1 and p_2, respectively. The values of D_a represent local effective diffusion coefficients averaged over the concentration interval from C_1 to C_2. In the low-pressure permeation experiments the diffusion coefficients, D, were estimated from the time lag according to the classical Daines−Barrer method:[46]

$$D = l^2/6\theta \tag{16}$$

where l is film thickness and θ is the time lag obtained from extrapolation of the steady-state line of the experimental permeation curve to the time axis.

No pressure dependence was noted in subatmospheric measurements of the diffusion coefficients of light gases (O_2, N_2, CO, CO_2, CH_4, SO_2) in the temperature range from 19 to 50 °C. The Arrhenius plots in Figure 10 were used to determine the E_D values in Table 6. Figure 11 presents D_a as a function of penetrant concentration in AF1600. For light gases the concentration dependence of D_a is very weak; however, it becomes more pronounced for larger, more soluble penetrants such as ethane and perfluoroethane. This result, in conjunction with the solubility data, indicates that the dramatic increase in permeability observed for these penetrants with increasing Δp is caused primarily by increased penetrant mobility.

The diffusion coefficients in AF1600 obtained by both methods are shown in Figure 12 as a function of penetrant size. Corresponding data for AF2400 are also presented. Reasonable agreement between the pressure-independent D and pressure-averaged D_a values was obtained. The latter are somewhat larger, and this can be a manifestation of the concentration dependence of D_a observed even for lightest gases (Figure 11). The diffusion coefficients in AF1600 are 3−4 times smaller than those in AF2400. This result is consistent with the smaller free volume of AF1600. In comparison to conventional glassy polymers like poly(vinyl chloride)

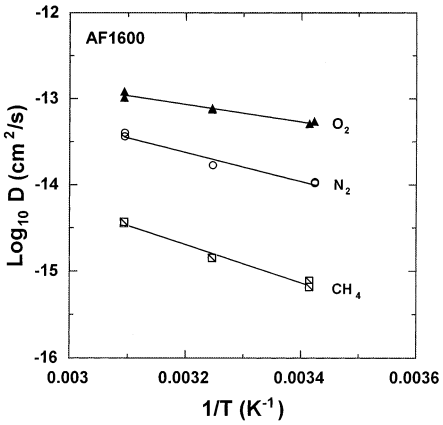

Figure 10. Arrhenius dependence for diffusion coefficients in AF1600.

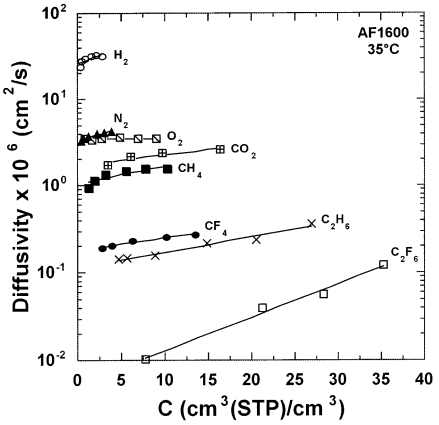

Figure 11. Effect of concentration on diffusion coefficients in AF1600 at 35 °C.

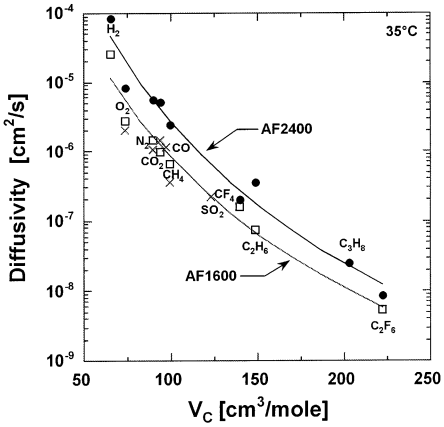

Figure 12. Correlation of infinite dilution gas diffusion coefficients with their critical volumes at 35 °C in AF2400(*4*) (●) and AF1600. In AF1600, the infinite dilution diffusion coefficients were determined either by high-pressure permeation and sorption measurements (□) or by the time-lag method (×).

[PVC] that are distinguished by low diffusivity but high diffusivity selectivity, AF1600 and AF2400 are weakly size sieving. Nevertheless, they have a much greater ability to separate molecules on the basis of size than PTMSP, an extraordinarily high free volume polymer that exhibits high diffusion coefficients and very low diffusivity selectivity,[15] and thus can be considered intermediate size sieving materials.

Conclusions

The solubility of a series of gases and vapors ranging in critical temperature from 126 to 659 K was studied via pressure decay and inverse gas chromatography. Good agreement between sorption measurement techniques was obtained. The linear correlations log S vs T_c^2 or log S vs $(T_c/T)^2$ were found to describe penetrant solubility in AF1600 better than traditional correlations with T_c. The penetrant solubility in AF1600 is lower than that in AF2400, consistent with the lower free volume of the former material. The solubility of perfluorinated compounds studied is higher in AF1600 than that of their hydrocarbon analogues, indicative of more favorable interactions of perfluorocarbons with the chemically similar polymer matrix.

The free volume in AF1600 was studied using positron annihilation lifetime spectroscopy. Similar to other high free volume polymers, a bimodal size distribution of free volume elements is observed for AF1600. The larger free volume elements have a radius of approximately 5 Å. Microcavity volume distributions measured by PALS and IGC methods for three polymers, AF1600, AF2400, and PVTMS, were found to be similar.

Permeability and diffusion coefficients of AF1600 decrease as penetrant size increases. AF1600 is easily plasticized by the larger, more soluble penetrants examined. In comparison to AF2400, P and D values are lower in AF1600, consistent with a lower perfluorodioxole [BDD] content that results in more efficient chain packing and lower free volume for this copolymer. Permeation rates of all gases in AF1600 except CO_2 increase with temperature, indicating activation energies of permeation are positive (other than carbon dioxide). It should be mentioned, however, that activation energies E_P and E_D in AF1600 are relatively small as compared with those of conventional glassy polymers. This result indicates that penetrants make diffusive jumps relatively easily in AF1600.

Acknowledgment. The research described in this article was made possible in part by Award No. RC2-347 of the US Civilian Research and Development Foundation for the Independent States of the Former Soviet Union (CRDF) and by Grant CTS98-03225 from the National Science Foundation.

References and Notes

(1) Nemser, S. M.; Roman, I. C. US Patent 5 051 114, 1991.
(2) Pinnau, I.; Toy, L. G. *J. Membr. Sci.* **1996**, *109*, 125−133.
(3) Alentiev, A. Y.; Yampolskii, Y. P.; Shantarovich, V. P.; Nemser, S. M.; Platé, N. A. *J. Membr. Sci.* **1997**, *126*, 123−132.
(4) Merkel, T. C.; Bondar, V.; Nagai, K.; Freeman, B. D.; Yampolskii, Y. P. *Macromolecules* **1999**, *32*, 8427−8440.
(5) Hildebrand, J. H.; Prausnitz, J. M.; Scott, R. L. *Regular and Related Solutions: The Solubility of Gases, Liquids, and Solids*; Van Nostrand Reinhold: New York, 1970.
(6) Meares, P. *J. Am. Chem. Soc.* **1954**, *76*, 3415−3422.
(7) Merkel, T. C.; Bondar, V.; Nagai, K.; Freeman, B. D. *Macromolecules* **1999**, *32*, 370−374.
(8) Stern, S. A. *J. Membr. Sci.* **1994**, *94*, 1−65.
(9) Resnick, P. R.; Buck, W. H. In *Modern Fluoropolymers: High Performance Polymers for Diverse Applications*; Scheirs, J., Ed.; John Wiley & Sons: New York, 1997; pp 397−419.
(10) Pixton, M. R.; Paul, D. R. In *Polymeric Gas Separation Membranes*; Paul, D. R., Yampolskii, Yu. P., Eds.; CRC Press: Boca Raton, FL, 1994; pp 83−153.
(11) Yampolskii, Y. P.; Bespalova, N. B.; Finkelshtein, E. S.; Bondar, V. I.; Popov, A. V. *Macromolecules* **1994**, *27*, 2872.
(12) Tanaka, K.; Okano, M.; Toshino, M.; Kita, H.; Okamoto, K. *J. Polym. Sci., Part B: Polym. Phys.* **1992**, *30*, 907.
(13) Pauly, S. In *Polymer Handbook*, 3rd ed.; Brandrup, E. J., Immergut, E. H., Eds.; John Wiley and Sons: New York, 1989; pp VI/435−VI/449.
(14) Masuda, T.; Isobe, E.; Higashimura, T.; Takada, K. *J. Am. Chem. Soc.* **1983**, *105*, 7473.
(15) Merkel, T. C.; Bondar, V.; Nagai, K.; Freeman, B. D. *J. Polym. Sci., Part B: Polym. Phys.* **2000**, *38*, 273−296.
(16) Bondar, V. I.; Freeman, B. D.; Yampolskii, Y. P. *Macromolecules* **1999**, *32*, 6163−6171.
(17) Squire, E. N. US Patent 4 754 009, 1988.
(18) Stern, S. A.; Gareis, P. J.; Sinclair, T. F.; Mohr, P. H. *J. Appl. Polym. Sci.* **1963**, *7*, 2035.
(19) Yampolskii, Y.; Novitskii, E.; Durgayan, S. *Zavodsk. Lab.* **1980**, *46*, 256.
(20) Koros, W. J.; Chern, R. T. In *Handbook of Separation Process Technology*; Rousseau, R. W., Ed.; John Wiley & Sons: New York, 1987; pp 862−953.
(21) El-Hibri, M.; Paul, D. R. *J. Appl. Polym. Sci.* **1986**, *31*, 2533.
(22) Paterson, R.; Yampolskii, Y.; Fogg, P. G. T. Solubility of Gases in Glassy Polymers, IUPAC/NIST SDS Series, V.70; *J. Phys. Chem. Ref. Data* **1999**, *28*, 1255.
(23) Fleming, G. K.; Koros, W. J. *Macromolecules* **1986**, *19*, 2285.
(24) Toi, K.; Morel, G.; Paul, D. R. *J. Appl. Polym. Sci.* **1982**, *27*, 2997.
(25) Chern, R. T.; Koros, W. J.; Hopfenberg, H. B.; Stannett, V. T. *J. Polym. Sci.: Part B: Polym. Phys.* **1984**, *22*, 1061.
(26) Scharlin, P.; Battino, R.; Silla, E.; Tunon, I.; Pascual-Ahular, J. L. *Pure Appl. Chem.* **1998**, *70*, 1895−1904.
(27) Shantarovich, V. P.; Kevdina, I. B.; Yampolskii, Y. P.; Alentiev, A. Y. *Macromolecules* **2000**, *33*, 7453−7466.
(28) Yampolskii, Y.; Korikov, A.; Shantarovich, V.; Nagai, K.; Freeman, B. D.; Masuda, T.; Teraguchi, M.; Kwak, G. *Macromolecules* **2001**, *34*, 1788−1796.
(29) Kawakami, M.; Kagawa, S. *Bull. Chem. Soc. Jpn.* **1978**, *51*, 75.
(30) Stern, S. A.; Mullhaupt, J. T.; Gareis, P. J. *AIChE J.* **1969**, *15*, 64−73.
(31) Suwandi, M. S.; Stern, S. A. *J. Polym. Sci., Polym. Phys. Ed.* **1973**, *11*, 663−681.
(32) Soloviev, S. A.; Yampolskii, Y. P.; Economou, I. G.; Ushakov, N. V.; Finkelshtein, E. S. *Vysokomol. Soedin.* **2002**, *44*, 465−473.
(33) Merkel, T. C.; Bondar, V. I.; Nagai, K.; Freeman, B. D.; Pinnau, I. *J. Polym. Sci., Part B: Polym. Phys.* **2000**, *38*, 415−434.
(34) Stull, D. R.; Westrum, E. F.; Sinke, G. C. *The Chemical Thermodynamics of Organic Compounds*; Wiley: New York, 1969.
(35) Yampolskii, Y. P.; Kaliuzhnyi, N. E.; Durgaryan, S. G. *Macromolecules* **1986**, *19*, 846.
(36) Nakanishi, H.; Wang, S. J.; Jean, Y. C. In *International Symposium on Positron Annihilation Studies of Fluids*; Sharma, S. C., Ed.; World Scientific: Singapore, 1987; p 292.
(37) Consolati, G.; Genco, I.; Pegoraro, M.; Zanderighi, L. *J. Polym. Sci., Part B: Polym. Phys.* **1996**, *34*, 357.
(38) Yampolskii, Y. P.; Shantorovich, V. P.; Chernyakovskii, F. P.; Kornilov, A. I.; Platé, N. A. *J. Appl. Polym. Sci.* **1993**, *47*, 85−92.
(39) Schmitz, H.; Mueller-Plathe, F. *J. Chem. Phys.* **2000**, *112*, 1040.
(40) Yampolskii, Y. P.; Durgaryan, S. G.; Nametkin, N. S. *Vysokomol. Soedin., B* **1979**, *21*, 616.
(41) Freeman, B. D.; Pinnau, I. In *Polymeric Membranes for Gas and Vapor Separations: Chemistry and Materials Science*; ACS Symposium Series No. 733; Freeman, B. D., Pinnau, I., Eds.; American Chemical Society: Washington, DC, 1999; pp 1−27.
(42) Masuda, T.; Iguchi, Y.; Tang, B.-Z.; Higashimura, T. *Polymer* **1988**, *29*, 2041.
(43) Pinnau, I.; Toy, L. G. *J. Membr. Sci.* **1996**, *116*, 199−209.
(44) Starannikova, L. E.; Teplyakov, V. V. *Vysokomol. Soedin., A* **1997**, *39*, 1690.
(45) Haraya, K.; Obata, K.; Hakuta, T.; Yoshitome, H. *Maku (Membrane)* **1986**, *11*, 48−52.
(46) Crank, J. *The Mathematics of Diffusion*, 2nd ed.; Clarendon Press: Oxford, 1975.

MA020494F